

# Benzo-21-crown-7-Based [1]Rotaxanes: Syntheses, X-ray Crystal Structures, and Dynamic Characteristics

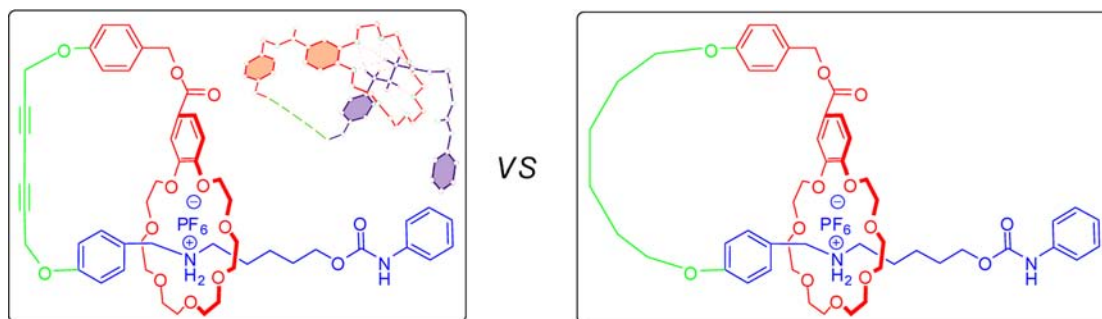
Qizhong Zhou,<sup>\*,†</sup> Peifa Wei,<sup>‡</sup> Yanyan Zhang,<sup>§</sup> Yihua Yu,<sup>§</sup> and Xuzhou Yan<sup>\*,‡</sup>

Department of Chemistry, Taizhou University, Taizhou, 318000, P. R. China,  
Department of Chemistry, Zhejiang University, Hangzhou 310027, P. R. China, and  
Shanghai Key Laboratory of Magnetic Resonance, Department of Physics, East China  
Normal University, Shanghai 200062 P. R. China

qizhongzhou@tzc.edu.cn; xzyan@zju.edu.cn

Received September 10, 2013

## ABSTRACT



Two B21C7-based [1]rotaxanes were synthesized in high yields by means of copper(II)-mediated Eglinton coupling and a subsequent Pd/C-catalyzed reduction under H<sub>2</sub>. X-ray single-crystal analysis shows that [1]rotaxane takes on a self-entangled conformation, wherein the macrocycle is threaded by its own tail. Moreover, it was found that [1]rotaxane with a flexible skeleton had more rotational motions than that of one with a rigid skeleton.

Supramolecular chemistry,<sup>1</sup> as chemistry beyond the molecule defined by Lehn, has developed quickly during the last several decades with the aim of constructing advanced supramolecular architectures with unique functions<sup>2</sup> and nontrivial topologies<sup>3</sup> by drawing inspiration

from nature. As a kind of intriguing supramolecular architecture, mechanically interlocked molecules (MIMs)<sup>4</sup> have captured the attention of the scientific community, not only because of their topological importance<sup>5</sup> but also because of their application in the construction of artificial molecular machines,<sup>6</sup> mechanically bonded polymers,<sup>7</sup> and other functional supramolecular entities.<sup>8</sup> [1]Rotaxanes, acting as the simplest MIMs, are self-entangled species

<sup>†</sup> Taizhou University.

<sup>‡</sup> Zhejiang University.

<sup>§</sup> East China Normal University.

(1) Lehn, J.-M. *Supramolecular Chemistry*; VCH: Weinheim, 1995.

(2) (a) Chen, S.-G.; Yu, Y.; Zhao, X.; Ma, Y.; Jiang, X.-K.; Li, Z.-T. *J. Am. Chem. Soc.* **2011**, *133*, 11124–11127. (b) Yan, X.; Wang, F.; Zheng, B.; Huang, F. *Chem. Soc. Rev.* **2012**, *41*, 6042–6065. (c) Yan, X.; Li, S.; Cook, T. R.; Ji, X.; Yao, Y.; Pollock, J. B.; Shi, Y.; Yu, G.; Li, J.; Huang, F.; Stang, P. J. *J. Am. Chem. Soc.* **2013**, *135*, 14036–14039.

(3) (a) Wang, F.; Zhang, J.; Ding, X.; Dong, S.; Liu, M.; Zheng, B.; Li, S.; Wu, L.; Yu, Y.; Gibson, H. W.; Huang, F. *Angew. Chem., Int. Ed.* **2010**, *49*, 1090–1094. (b) Li, S.; Huang, J.; Cook, T. R.; Pollock, J. B.; Kim, H.; Chi, K.-W.; Stang, P. J. *J. Am. Chem. Soc.* **2013**, *135*, 2084–2087. (c) Yan, X.; Li, S.; Pollock, J. B.; Cook, T. R.; Chen, J.; Zhang, Y.; Ji, X.; Yu, Y.; Huang, F.; Stang, P. J. *Proc. Natl. Acad. Sci. U.S.A.* **2013**, *110*, 15585–15590.

(4) (a) Amabilino, D. B.; Stoddart, J. F. *Chem. Rev.* **1995**, *95*, 2725–2828. (b) Hu, X.; Chen, L.; Si, W.; Yu, Y.; Hou, J.-L. *Chem. Commun.* **2011**, *47*, 4694–4696. (c) Zhang, Z.; Han, C.; Yu, G.; Huang, F. *Chem. Sci.* **2012**, *3*, 3026–3031.

(5) Forgan, R. S.; Sauvage, J.-P.; Stoddart, J. F. *Chem. Rev.* **2011**, *111*, 5434–5464.

(6) (a) Kay, E. R.; Leigh, D. A.; Zerbetto, F. *Angew. Chem., Int. Ed.* **2007**, *46*, 72–191. (b) Silvi, S.; Venturi, M.; Credi, A. *Chem. Commun.* **2011**, *47*, 2483–2489. (c) Zhu, K.; Vukotic, V. N.; Loeb, S. J. *Angew. Chem., Int. Ed.* **2012**, *51*, 2168–2172. (d) Baroncini, M.; Silvi, S.; Venturi, M.; Credi, A. *Angew. Chem., Int. Ed.* **2012**, *51*, 4223–4226. (e) Yan, X.; Wei, P.; Li, Z.; Zheng, B.; Dong, S.; Huang, F.; Zhou, Q. *Chem. Commun.* **2013**, *49*, 2512–2514.

(7) (a) Niu, Z.; Gibson, H. W. *Chem. Rev.* **2009**, *109*, 6024–6046. (b) Li, S.; Zheng, B.; Chen, J.; Dong, S.; Ma, Z.; Huang, F.; Gibson, H. W. *J. Polym. Sci., Part A: Polym. Chem.* **2010**, *48*, 4067–4073.

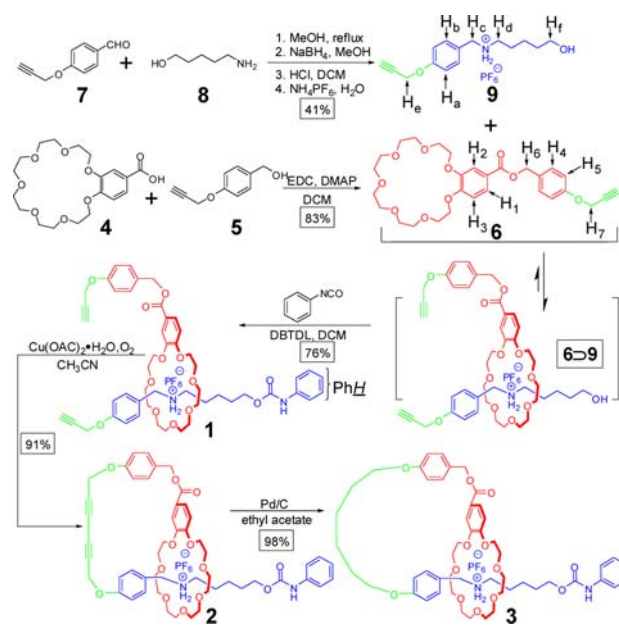
(8) (a) Ji, X.; Yao, Y.; Li, J.; Yan, X.; Huang, F. *J. Am. Chem. Soc.* **2013**, *135*, 74–77. (b) Yan, X.; Zheng, B.; Huang, F. *Polym. Chem.* **2013**, *4*, 2395–2399.

wherein the macrocycle and the axle part are covalently bound together.<sup>9</sup> Due to their rather unique and intriguing structures, a variety of host–guest recognition motifs have been exploited for the preparation of [1]rotaxanes. For example, Easton and co-workers reported the first cyclodextrin (CD)-based [1]rotaxane starting from a [2]rotaxane by fixing a covalent linkage between the CD ring and the stilbene axis.<sup>10</sup> Later, Tian et al. reported a fully optical CD-based [1]rotaxane by self-complementary and subsequent Suzuki-coupling capping.<sup>11</sup> Furthermore, the same group prepared a light-powered symmetric [1]rotaxane which can act as a molecular muscle by inducing reversible stretch-contraction at the molecular level.<sup>12</sup> In 2004, Hiratani et al. synthesized a [1]rotaxane via covalent bond formation which showed unique fluorescent response by energy transfer in the presence of a lithium ion.<sup>13</sup> Subsequently, Mayer et al. reported on a system that can be interconverted between a disentangled and a self-entangled [1]rotaxane conformation under appropriate chemically stimulated conditions.<sup>9</sup> Recently, Qu and co-workers reported two ferrocene-based bistable [1]rotaxanes that exhibited interesting electrochemical or fluorescent signal output, respectively.<sup>14</sup> All of these investigations have opened up new exciting possibilities for the applications of [1]rotaxanes.

In 2007, Huang's group found that benzo-21-crown-7 (B21C7) can bind dialkylammonium salts to form threaded structures.<sup>15</sup> Since the cavity of B21C7 is smaller than the traditional crown ether host dibenzo-24-crown-8 (DB24C8), it not only binds dialkylammonium salts more strongly but also needs simpler and smaller stoppers (for example benzene ring) for the preparation of MIMs. On account of these virtues, this recognition motif has been widely employed to prepare various threaded systems. For example, Huang and co-workers reported the construction of B21C7-based supramolecular polymeric materials.<sup>16</sup> Schalley et al. constructed hetero[n]rotaxanes ( $n = 3$  or 4) by integrative self-sorting.<sup>17</sup> Liu et al. synthesized a twin-axial hetero[7]rotaxane.<sup>18</sup> However, up to now, no [1]rotaxanes have been reported on the basis of this

recognition motif, although they represent a kind of appealing structures. Herein, we report the efficient syntheses of two B21C7-based [1]rotaxanes (one with a rigid skeleton and the other with a flexible skeleton) and the formation of interesting self-assembly [1]rotaxane structures in the solid state. Furthermore, their dynamic characteristics were investigated by variable-temperature <sup>1</sup>H NMR.

**Scheme 1.** Synthetic Strategy for the Preparation of [1]Rotaxanes **2** and **3**



As outlined in Scheme 1, the strategy employed to synthesize [1]rotaxanes **2** and **3** is based on copper(II)-mediated Eglinton coupling on a [2]rotaxane **1** with propargyl groups and a subsequent Pd/C-catalyzed reduction under H<sub>2</sub>. Secondary ammonium salt **9** was obtained in 41% total yield for the four steps (condensation, reduction, protonation, and counterion exchange) from commercial available 4-(prop-2-yn-1-yloxy)benzaldehyde **7** and 5-amino-1-pentanol **8**. B21C7 derivative **6** was obtained by esterification between **4** and **5**. Guest **9** was slightly soluble in CH<sub>2</sub>Cl<sub>2</sub>. However, it became soluble after the addition of equimolar host **6**, showing the formation of [2]semirotaxane **6**⊃**9**. Mixing host **6**, guest **9**, phenyl isocyanate, and a catalytic amount of dibutyltin dilaurate (DBTDL) in CH<sub>2</sub>Cl<sub>2</sub> followed by stirring at room temperature for 2 days afforded [2]rotaxane **1** in 76% isolated yield. Subsequently, [1]rotaxane **2** was prepared in 91% isolated yield by slow addition of the dialkyne [2]rotaxane **1** to an acetonitrile solution of Cu(OAc)<sub>2</sub> under O<sub>2</sub> at 45 °C. Finally, [1]rotaxane **3** was synthesized in 98% yield by Pd/C-catalyzed reduction of [1]rotaxane **2** under H<sub>2</sub> atmosphere. Therefore, we developed a novel and high-yielding method to synthesize crown ether-based [1]rotaxanes.

(9) Xue, Z.; Mayer, M. F. *J. Am. Chem. Soc.* **2010**, *132*, 3274–3276.

(10) Onagi, H.; Blake, C. J.; Easton, C. J.; Lincoln, S. F. *Chem.—Eur. J.* **2003**, *9*, 5978–5988.

(11) Ma, X.; Qu, D.; Ji, F.; Wang, Q.; Zhu, L.; Xu, Y.; Tian, H. *Chem. Commun.* **2007**, 1409–1411.

(12) Gao, C.; Ma, X.; Zhang, Q.; Wang, Q.; Qu, D.; Tian, H. *Org. Biomol. Chem.* **2011**, *9*, 1126–1132.

(13) Hiratani, K.; Kaneyama, M.; Nagawa, Y.; Koyama, E.; Kanesato, M. *J. Am. Chem. Soc.* **2004**, *126*, 13568–13569.

(14) (a) Li, H.; Zhang, H.; Zhang, Q.; Zhang, Q.-W.; Qu, D.-H. *Org. Lett.* **2012**, *14*, 5900–5903. (b) Li, H.; Zhang, J.-N.; Zhou, W.; Zhang, H.; Zhang, Q.; Qu, D.-H.; Tian, H. *Org. Lett.* **2013**, *15*, 3070–3073.

(15) Zhang, C.; Li, S.; Zhang, J.; Zhu, K.; Li, N.; Huang, F. *Org. Lett.* **2007**, *9*, 5553–5556.

(16) (a) Yan, X.; Zhou, M.; Chen, J.; Chi, X.; Dong, S.; Zhang, M.; Ding, X.; Yu, Y.; Shao, S.; Huang, F. *Chem. Commun.* **2011**, 7086–7088. (b) Yan, X.; Xu, D.; Chi, X.; Chen, J.; Dong, S.; Ding, X.; Yu, Y.; Huang, F. *Adv. Mater.* **2012**, *24*, 362–369. (c) Chen, L.; Tian, Y.-K.; Ding, Y.; Tian, Y.-J.; Wang, F. *Macromolecules* **2012**, *45*, 8412–8419. (d) Yan, X.; Xu, D.; Chen, J.; Zhang, M.; Hu, B.; Yu, Y.; Huang, F. *Polym. Chem.* **2013**, *4*, 3312–3322.

(17) (a) Jiang, W.; Winkler, H. D. F.; Schalley, C. A. *J. Am. Chem. Soc.* **2008**, *130*, 13852–13853. (b) Jiang, W.; Sattler, D.; Rissanen, K.; Schalley, C. A. *Org. Lett.* **2011**, *13*, 4502–4505.

(18) Zhang, Z.-J.; Zhang, H.-Y.; Wang, H.; Liu, Y. *Angew. Chem., Int. Ed.* **2011**, *50*, 10834–10838.

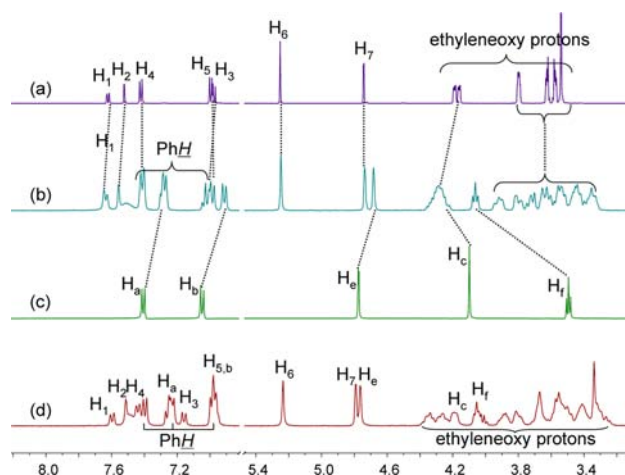


**Figure 1.** Partial  $^1\text{H}$  NMR spectra (500 MHz,  $\text{CD}_3\text{CN}$ , 293 K) of (a) 5.00 mM **6**; (b) 5.00 mM **1**; (c) 5.00 mM **9**; (d) 5.00 mM **1** in  $\text{DMSO}-d_6$ .

Partial proton  $^1\text{H}$  NMR spectra of host **6**, guest **9**, and [2]rotaxane **1** are shown in Figure 1. The aromatic protons  $\text{H}_1$ ,  $\text{H}_2$ , and  $\text{H}_3$  of host **6** moved downfield after the formation of [2]rotaxane **1** (Figure 1, spectra a and b). Meanwhile,  $\text{H}_a$  and  $\text{H}_b$  on guest **9** showed a significant upfield shift (Figure 1, spectra b and c), which may due to the strong shielding effect of the crown ether ring. To further prove the formation of MIM, [2]rotaxane **1** was dissolved in  $\text{DMSO}-d_6$  since no complexation occurred in this highly polar solvent. The  $^1\text{H}$  NMR spectrum of **1** in  $\text{DMSO}-d_6$  (Figure 1, spectrum d) showed complicated peaks as observed in  $\text{CD}_3\text{CN}$  (Figure 1, spectrum b), indicating the existence of [2]rotaxane **1**. Moreover, electrospray ionization mass spectrum (ESI-MS) of [2]rotaxane **1** showed a strong single peak at  $m/z$  911.8 (100%) corresponding to  $[\mathbf{1} - \text{PF}_6]^+$  (Figure S9, Supporting Information), indicating the [2]rotaxane formation.

Copper(II)-mediated Eglinton coupling on [2]rotaxane **1** yielded [1]rotaxane **2** with a rigid skeleton<sup>19</sup> and a subsequent Pd/C-catalyzed reduction of **2** under  $\text{H}_2$  gave [1]rotaxane **3** with a flexible skeleton. The formation of [1]rotaxanes **2** and **3** were both confirmed by ESI-MS:  $m/z$  909.8 (100%) corresponding to  $[\mathbf{2} - \text{PF}_6]^+$  (Figure S12, Supporting Information) and  $m/z$  917.9 (100%) corresponding to  $[\mathbf{3} - \text{PF}_6]^+$  (Figure S15, Supporting Information). After the formation of [1]rotaxane **2** from [2]rotaxane **1**, the dynamic molecular motions of **1** were found to be somewhat restricted. As shown in Figure 2, the ethyleneoxy protons corresponding to each  $-\text{OCH}_2-$  unit on the “wheel” of [1]rotaxane **2** (Figure 2, spectrum b) were well recognized compared to that of [2]rotaxane **1** (Figure 2, spectrum a). Meanwhile, methylene protons  $\text{H}_6$  on [1]rotaxane **2** were observed to split into two sets of double peaks (Figure 2, spectrum b) from a single peak (Figure 2,

spectrum a) on [2]rotaxane **1**, indicating that the motion of  $\text{H}_6$  was suppressed and slow on the NMR time scale at room temperature. This can be attributed to restrict rotation of the “wheel” on [1]rotaxanes. Protons  $\text{H}_6$  located in the inner and outer spaces of the [1]rotaxane cavity were shielded and deshielded, respectively, leading to the 1:1 split.<sup>20</sup> Furthermore, the reduction of the rigid  $-\text{C}\equiv\text{C}-\text{C}\equiv\text{C}-$  fragment on [1]rotaxane **2** into flexible alkylchain yielded [1]rotaxane **3**. Although **3** had a more flexible structure and larger cavity, the splitting of  $\text{H}_6$  was also observed (Figure 2, spectrum c). But, it was found that ethyleneoxy protons on the “wheel” merged again to form more complicated peaks, indicating that restricted rotation on [1]rotaxane **3** was somewhat suppressed. Therefore, [1]rotaxanes **2** with a rigid skeleton and **3** with a flexible skeleton are good models for the investigation of rotational motions of MIMs.

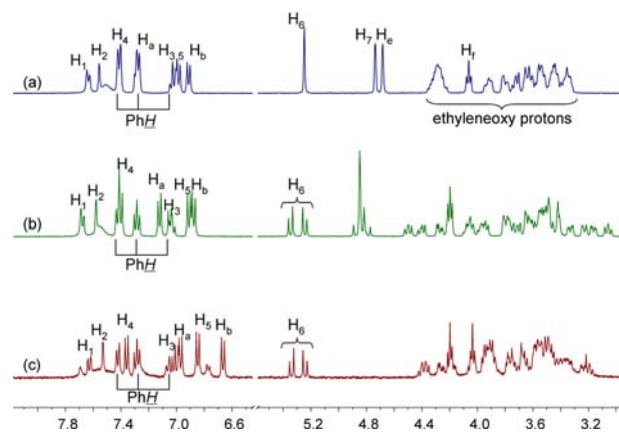


**Figure 2.** Partial  $^1\text{H}$  NMR spectra (500 MHz,  $\text{CD}_3\text{CN}$ , 293 K) of (a) 5.00 mM [2]rotaxane **1**; (b) 5.00 mM [1]rotaxane **2**; (c) 5.00 mM [1]rotaxane **3**.

In order to visualize the structure of [1]rotaxanes, a colorless single crystal of [1]rotaxane **2** was obtained by a vapor diffusion method, but all attempts to grow X-ray quality single crystals of [1]rotaxane **3** were proven to be unsuccessful because of its relatively flexible structure. The X-ray crystal structure of **2** shows that [1]rotaxane takes on a self-entangled conformation in which the macrocycle is threaded by its own tail (Figure 3a). Meanwhile, due to the existence of a diyne fragment on **2**, its left part has a relatively rigid skeleton. In the solid state, two  $N$ -H hydrogens and four  $N$ -methylene hydrogens of the axle component are involved in eleven hydrogen bonds ( $[\text{N}-\text{H}\cdots\text{O}]$ , a–d and  $[\text{C}-\text{H}\cdots\text{O}]$ , e–k, Figure 3a) with all oxygen atoms of the B21C7 part. It is worth noting that the number of hydrogen bonds (11 H-bonds) in this [1]rotaxane is more than that of the B21C7-based [2]rotaxane (9 H-bonds) reported by Huang and

(19) Miljanić, O. Š.; Dichtel, W. R.; Khan, S. I.; Mortezaei, S.; Heath, J. R.; Stoddart, J. F. *J. Am. Chem. Soc.* **2007**, *129*, 8236–8246.

(20) (a) Han, C.; Ma, F.; Zhang, Z.; Xia, B.; Yu, Y.; Huang, F. *Org. Lett.* **2010**, *12*, 4360–4363. (b) Zhang, Z.; Xia, B.; Han, C.; Yu, Y.; Huang, F. *Org. Lett.* **2010**, *12*, 3285–3287.



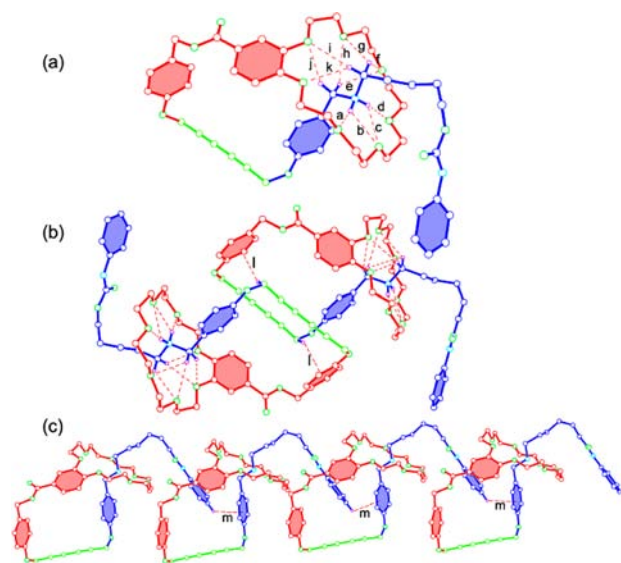


**Figure 3.** (a) Ball-stick view of the X-ray crystal structure of [1]rotaxane **2**. Host part is red, guest part is blue, diyne fragment is green, hydrogens are purple, oxygens are green, and nitrogens are sky blue.  $\text{PF}_6^-$  counterion and hydrogens except the ones involved in hydrogen bonding were omitted for clarity. Hydrogen bond parameters are as follows: H···O distance (Å), C···O distance (Å), C–H···O angle (deg): a, 1.20, 2.89, 164; b, 2.43, 2.90, 112; c, 2.53, 2.90, 105; d, 2.02, 2.93, 168; e, 2.05, 3.39, 132; f, 2.64, 3.36, 130; g, 2.56, 3.29, 131; h, 2.70, 3.29, 118; i, 2.62, 3.42, 139; j, 2.57, 3.46, 150; k, 2.66, 3.46, 138. (b) Parameters of C–H··· $\pi$  interaction (l) in the dimer structure of **2**: an H···phenyl ring centroid distance (Å) of 2.70 and a C···centroid distance (Å) of 3.26. (c) Linear [1]rotaxane superstructure in the solid state driven by edge-to-face  $\pi$ -stacking interactions. An H···phenyl ring centroid distance (Å) of 2.86 and a C···centroid distance (Å) of 3.44 (m).

co-workers,<sup>15</sup> indicating that restricting rotational motion of the macrocyclic component in MIMs is in favor of the formation of hydrogen bonds. Furthermore, driven by C–H··· $\pi$  interactions (l), a dimer structure of [1]rotaxane **2** is found in the solid state (Figure 3b). More interestingly, in the packing state, a linear [1]rotaxane superstructure forms driven by edge-to-face  $\pi$ -stacking interactions (m) (Figure 3c).

To further study the dynamic characteristics of [1]rotaxanes **2** and **3**, variable-temperature  $^1\text{H}$  NMR experiments were performed from 233 to 348 K in  $\text{CD}_3\text{CN}$  (Figure 4). Methylene protons  $\text{H}_6$  on [1]rotaxane **2** kept the same splitting and did not show obvious changes in this temperature range (Figure 4a), indicating that the thermal motions of  $\text{H}_6$  were somewhat restricted due to the formation of the relatively rigid [1]rotaxane skeleton. At 298 K, protons  $\text{H}_6$  on **2** and **3** were the same on the NMR time scale. However, below or above this temperature, they were different. For example, from 233 to 348 K, the two sets of double peaks of  $\text{H}_6$  on [1]rotaxane **3** got near each other gradually. Upon heating to 348 K, the four peaks were almost coalescent together, indicating that the

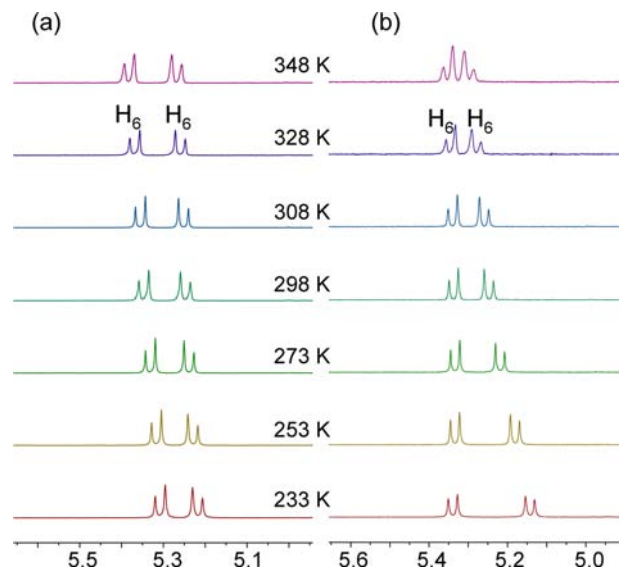


**Figure 4.** Partial variable-temperature  $^1\text{H}$  NMR spectra (500 MHz,  $\text{CD}_3\text{CN}$ ) of [1]rotaxane **2** (a) and [1]rotaxane **3** (b).

thermal motions of  $\text{H}_6$  on [1]rotaxane **3** were fast because of its flexible skeleton. These proved that protons  $\text{H}_6$  on [1]rotaxane **3** had more mobility than those of [1]rotaxane **2** due to their structural differences.

In summary, by means of copper(II)-mediated Eglinton coupling and a subsequent Pd/C-catalyzed reduction under  $\text{H}_2$ , two B21C7-based [1]rotaxanes **2** and **3** were synthesized in high yields. X-ray single crystal analysis shows that [1]rotaxane takes on a self-entangled conformation in which the macrocycle is threaded by its own tail. Interestingly, in the packing state, [1]rotaxane **2** further forms a dimer structure and a linear [1]rotaxane superstructure driven by C–H··· $\pi$  and edge-to-face  $\pi$ -stacking interactions, respectively. Moreover, due to their different structural characteristics, it was found that [1]rotaxane **3** with a flexible skeleton had more rotational motions than [1]rotaxane **2** with a rigid skeleton. On account of the unique dynamic characteristics of the present [1]rotaxanes, it would be promising for the incorporation of them into supramolecular polymeric scaffolds, because their integrated molecular motions would endow mechanically bonded polymeric materials with additional adaptability and intellectuality.

**Acknowledgment.** This work was supported by the National Natural Science Foundation of China (21172166) and China Postdoctor Foundation (2013M541456).

**Supporting Information Available.** Synthetic details, mass spectra, 2D COSY spectra, crystal data for **2**, and other materials. This material is available free of charge via the Internet at <http://pubs.acs.org>.

The authors declare no competing financial interest.